Atmospheric Deposition Studies of Microplastics in Central Germany

Sarmite Kernchen[1,2*], Holger Schmalz[3,4], Martin G. J. Löder[2], Christoph Georgi[5], Andrej Einhorn[1], Andreas Greiner[3,4], Anke C. Nölscher[1], Christian Laforsch[2] and Andreas Held[5]

[1]Chair of Atmospheric Chemistry, BayCEER, University of Bayreuth, Bayreuth, 95440, Germany
[2]Chair of Animal Ecology I, BayCEER, University of Bayreuth, Bayreuth, 95440, Germany
[3]Chair of Macromolecular Chemistry II, University of Bayreuth, Bayreuth, 95440, Germany
[4]Bavarian Polymer Institute, Keylab Synthesis and Molecular Characterization, University of Bayreuth, Bayreuth 95440, Germany
[5]Chair of Environmental Chemistry and Air Research, Technische Universität Berlin, Berlin, 10623, Germany
[*] Present address

Corresponding author: Sarmite Kernchen

Keywords: plastic pollution, wet, dry, and total deposition of microplastics, μFTIR, Raman spectroscopy

Supplementary Information

CONTENT

Mathematical equations: Dry deposition velocity calculations

Supermicron particles (> 1 µm) are expected to settle by sedimentation and due to turbulent motion. Therefore, the deposition velocity (*DV*) can be approximated by Eq. (1) [1]:

$$DV = \upsilon_s + \upsilon_t \quad (1)$$

where υ_s – particle sedimentation velocity (m s^{-1}); υ_t –turbulent dry deposition velocity (m s^{-1}). Depending on the particle equivalent spherical diameter (d_{ESD}) υ_t is approximated as 0.01 m s^{-1} for particles with d_{ESD} = 2.5-10 µm, 0.05 m s^{-1} for particles with d_{ESD} = 10-50 µm, and 0.2 m s^{-1} for particles with d_{ESD} larger than 50 µm [2].

The volume equivalent diameter d_{ESD} is the diameter for the sphere with the same volume as the particle under consideration, that is

$$d_{EDS} = \sqrt[3]{\frac{6V_p}{\pi}} \quad (2)$$

where V_p – particle volume; for calculation of V_p it was assumed that the particle is an elliptical cylinder with the major dimension *a*, minor dimension *b*, and height *h* (*a*, *b* determined by µFTIR).

$$V_p = \frac{1}{4}\pi abh \quad (3)$$

$$h = 0.67b \quad (4)$$

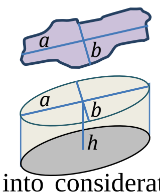

The sedimentation velocity υ_s was calculated by Newton's law of resistance (5), taking into consideration buoyancy effects and particle size and shape:

$$\upsilon_s = \sqrt{\frac{4}{3}\frac{d_{ESD}}{C_D}g\frac{\rho_p - \rho}{\rho}} \quad (5)$$

where C_D – dimensionless drag coefficient; *g* – gravitational acceleration (9.81 m s^{-1}); ρ – air density (1.225 kg m^{-3} or 1.225 × 10^9 µg m^{-3} at 1 atm and 15 °C); and ρ_p – particle density (µg m^{-3}).

The dimensionless drag coefficient was calculated following [3, 4] for non-spherical volcanic ash particles:

$$C_D = \frac{4}{3}\frac{0.559C_{D.\ sphere}(Re^{4.18}\psi^{-Re^{-0.2}})^{0.5134}}{Re^2} \quad (6)$$

$$C_{D.\ sphere} = \frac{24}{Re}(1 + 0.15Re^{0.687}) + \frac{0.42}{1+\frac{42500}{Re^{1.16}}} \quad (7)$$

$$\psi = \frac{\pi^{\frac{1}{3}}6V_p^{\frac{2}{3}}}{A_p} \quad (8)$$

$$Re = \frac{\rho\upsilon d}{\mu} \quad (9)$$

$$\upsilon = \frac{2(\rho_p - \rho) g (\frac{d}{2})^2}{9\mu} \qquad (10)$$

where *Re* – Reynolds number; ψ – sphericity; V_p – particle volume (m^3); A_p – particle surface area (m^2); μ is the dynamic viscosity of the air (1.81 kg m^{-1} s^{-1} or 1.81 × 10^9 µg m^{-1} s^{-1} at 15 °C); and υ – Stokes particle settling velocity (m s^{-1}).

Table S1: Wet and dry atmospheric deposition collection and meteorological data*

Parameter	May 29.04.19-27.05.19	June 27.05.19-24.06.19	July 24.06.19-29.07.19	August 29.07.19-27.08.19	September 27.08.19-30.09.19	October 30.09.19-30.10.19	November 30.10.19-26.11.19	December 26.11.19-02.01.20	Mean	SD
MP Dry DFs [N m^{-2} day^{-1}]	0	0	0	17	21	8	0	7	7	8
MP Wet DFs [N m^{-2} day^{-1}]	6	13	5	19	16	6	7	5	10	6
MP Total DFs [N m^{-2} day^{-1}]	6	13	5	37	39	15	7	13	17	14
MP conc. in precipitation [MPs L^{-1}]	2	9	5	12	18	3	6	3	7	5
Average dry period [days]	1.3	1.5	1.5	0.7	0.8	0.8	0.7	0.7	1	0
Maximal dry period [days]	5.8	5.4	7.5	4	4.4	6.7	6.3	7.5	6	1
Average wet period [h]	3.8	2.3	2.1	1.6	1.9	3	2.2	2.7	2	1
Maximal wet period [h]	16	6	5	7	8	11	14	16	10	5
Precipitation [mm]	93	40	39	48	32	57	33	66	51	21
Light rain (0.2-0.5 mm h^{-1}) [h]	9	8	12	25	32	22	24	35	21	10
Moderate rain (0.5-4.0 mm h^{-1}) [h]	8	10	9	12	7	8	9	12	9	2
Heavy rain (4.0-24 mm h^{-1}) [h]	1	0	0	0	0	0	0	0	0	0
Average rain intensity [mm h^{-1}]	0.88	0.82	0.7	0.49	0.28	0.48	0.36	0.36	1	0
Wind speed [m s^{-1}]	1.8	1.7	1.5	1.6	1.6	2.1	1.8	2.1	2	0
Average wind direction [°]	358	177	354	202	215	196	187	204	-	-
Dominant wind direction	NE	SSW	NE	SSW	SSW	SSW	SSW	SSW	-	-
TAPD** [km^{-2}]	294	331	308	325	351	286	297	295	311	23
Temperature [°C]	12	19	21	20	16	12	5	5	14	6
Global radiation [W m^{-2}]	179	231	223	189	133	58	27	16	132	87
Air pressure [hPa]	1016	1016	1018	1017	1019	1014	1007	1013	1015	4
Relative humidity [%]	73	68	67	68	74	85	91	88	77	10
PM10 [µg m^{-3}]	14	14	16	15	14	14	17	17	15	1
SO_2 [µg m^{-3}]	0.8	0.8	0.9	0.8	0.8	0.8	0.9	0.9	1	0
NO [µg m^{-3}]	2.3	1.9	2.1	2.4	3.8	5.6	9.6	9.4	5	3
NO_2 [µg m^{-3}]	15	15	14	16	19	20	26	26	19	5
O_3 [µg m^{-3}]	65	69	69	60	48	33	21	30	49	19

* Meteorological data were retrieved from wastewater treatment plant *KASSELWASSER* and weather station Kassel-Mitte (HLNUG)**;** ** Trajectory-averaged population density

Table S2: Correlation between meteorological variables and microplastic dry, wet, and total DFs, and concentrations in precipitation*

Parameter	MP dry DF [MPs m^{-2} day^{-1}]	MP wet DF [MPs m^{-2} day^{-1}]	MP total DF [MPs m^{-2} day^{-1}]	MP conc. in precipitation [MPs L^{-1}]
Average dry period [days]	-0.56	-0.21	-0.42	-0.12
Maximal dry period [days]	-0.40	-0.96	-0.61	-0.68
Average wet period [h]	-0.09	-0.58	-0.40	-0.87
Maximal wet period [h]	0.16	-0.28	-0.05	-0.58
Precipitation [mm]	0.29	-0.41	-0.20	-0.78
Light rain (drizzle. 0.2-0.5 mm h^{-1}) [h]	0.68	0.08	0.54	0.26
Moderate rain (0.5-4.0 mm h^{-1}) [h]	0.24	-0.02	-0.07	0.06
Heavy rain (4.0-24 mm h^{-1}) [h]	-0.24	-0.17	-0.41	-0.58
Average rain intensity [mm h^{-1}]	-0.20	-0.14	-0.55	-0.39
Wind speed [m s^{-1}]	-0.04	-0.19	0.02	-0.55
Average wind direction [°]	0.19	-0.36	-0.29	-0.32
Trajectory-averaged population density [km^{-2}]	0.00	0.64	0.38	0.91
Temperature [°C]	0.17	0.09	0.03	0.34
Global radiation [W m^{-2}]	-0.31	0.04	-0.16	0.14
Air pressure [hPa]	-0.12	0.23	0.25	0.50
Relative humidity [%]	0.17	0.07	0.17	-0.09
PM10 [µg m^{-3}]	-0.23	-0.12	-0.35	0.06
SO_2 [µg m^{-3}]	-0.30	-0.48	-0.57	-0.16
NO [µg m^{-3}]	0.39	0.13	0.24	0.04
NO_2 [µg m^{-3}]	0.38	0.32	0.38	0.18
O_3 [µg m^{-3}]	-0.37	-0.20	-0.28	-0.07

***Spearman rank correlation coefficients between meteorological variables and MP DFs and concentrations in precipitation: $p < 0.05$ (in red), $p > 0.05$ (in black)

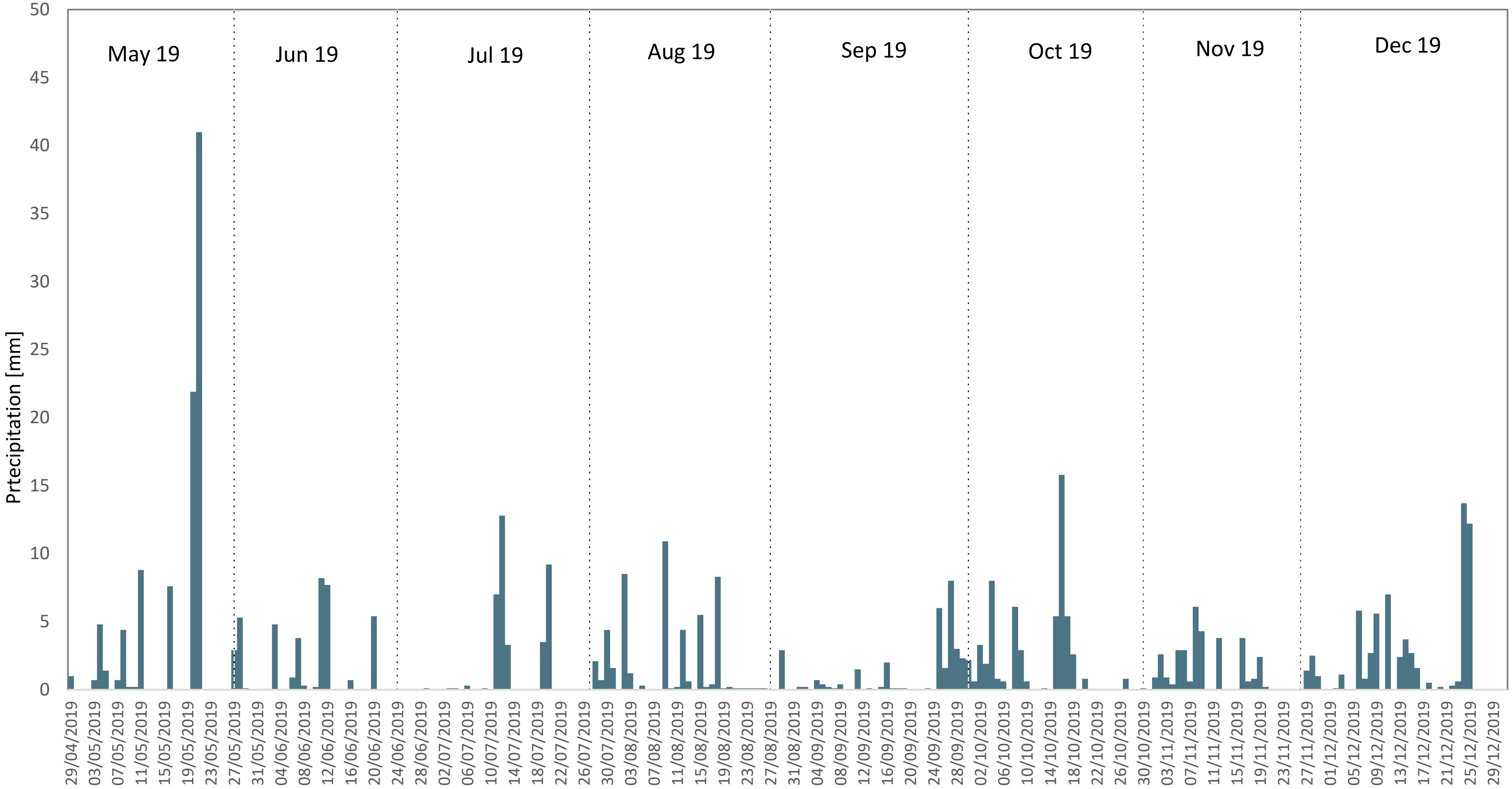

Figure S1: Daily precipitation at the sampling site in Kassel over monthly wet and dry deposition collection periods (indicated by vertical dotted lines). The data were retrieved from the wastewater treatment plant *KASSELWASSER*.

Figure S2: Wet and dry atmospheric deposition collector.

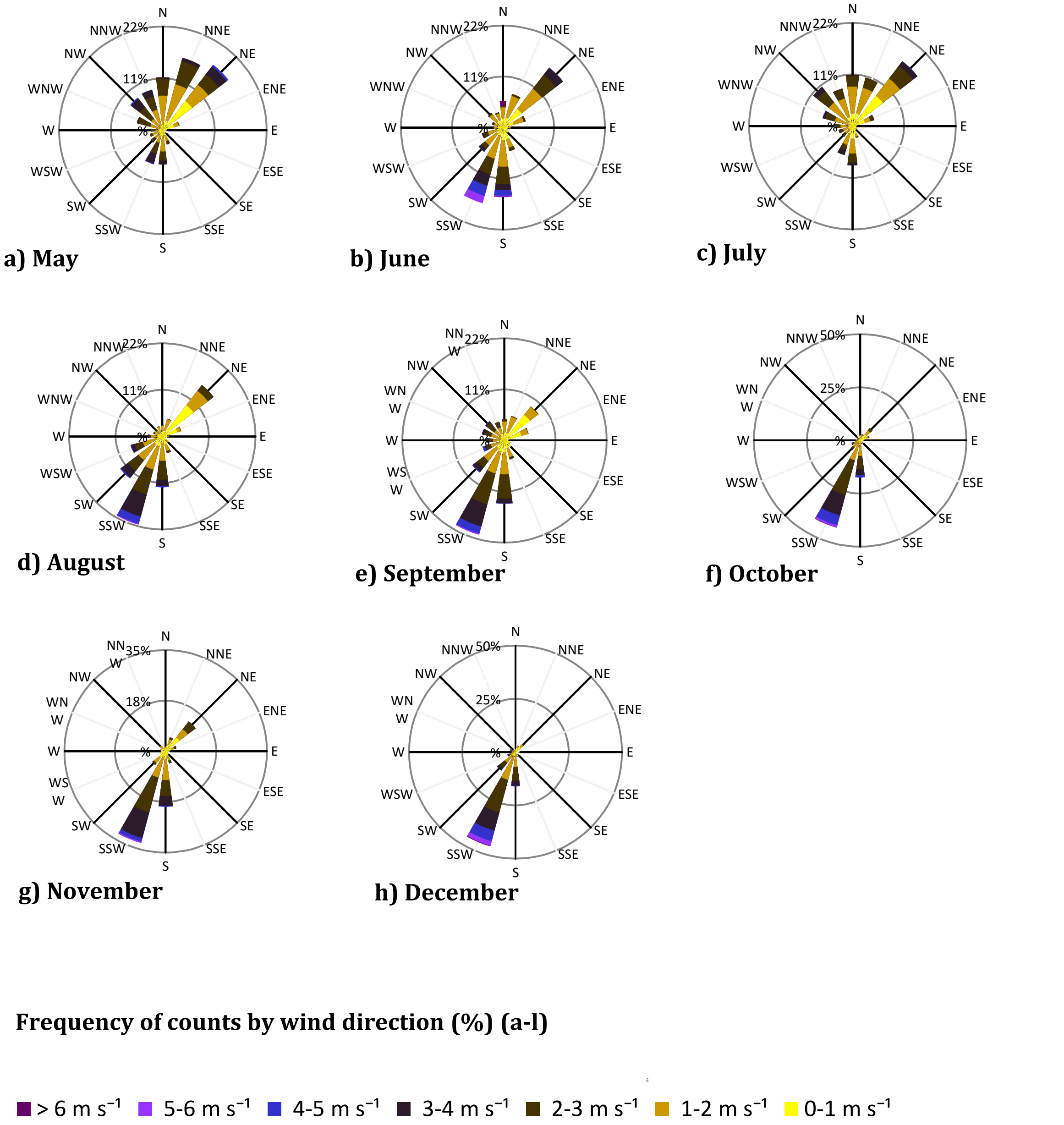

Figure S3a-l: Local wind field plots over the sampling period. Meteorological data were retrieved from the weather station Kassel-Mitte (HLNUG).

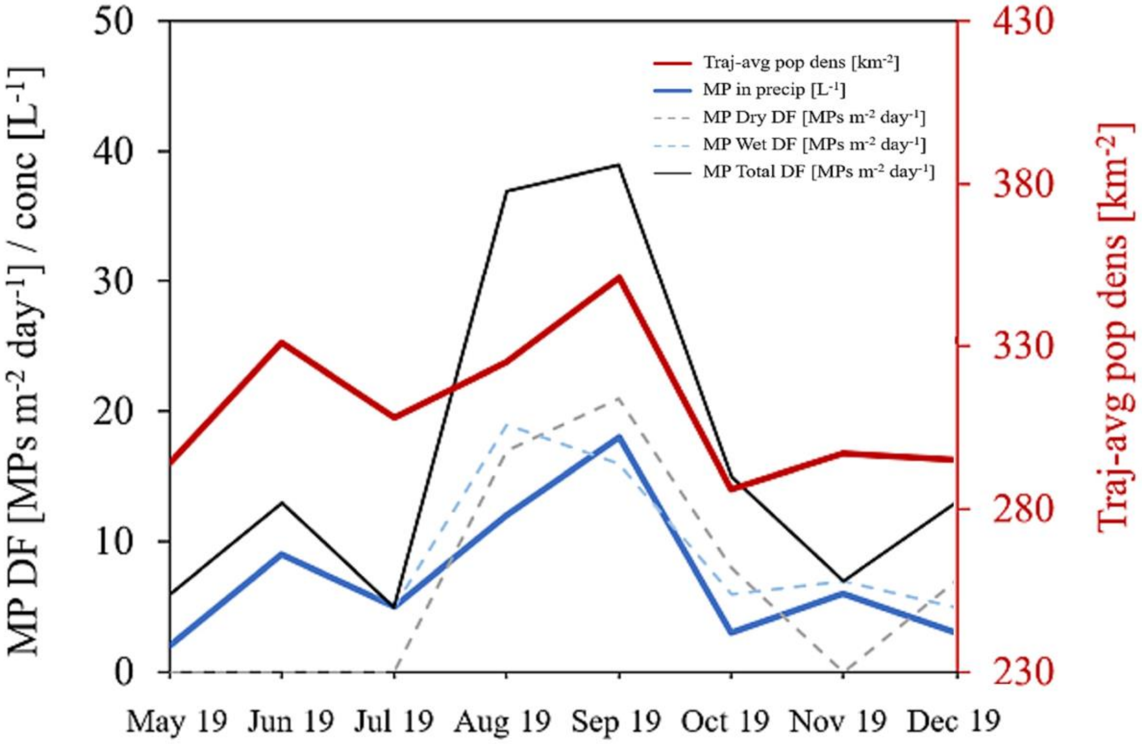

Figure S4: Temporal evolution of trajectory-averaged population density (red line), MP concentration in precipitation (blue line), and MP dry, wet and total DFs (broken grey and blue, solid black lines)

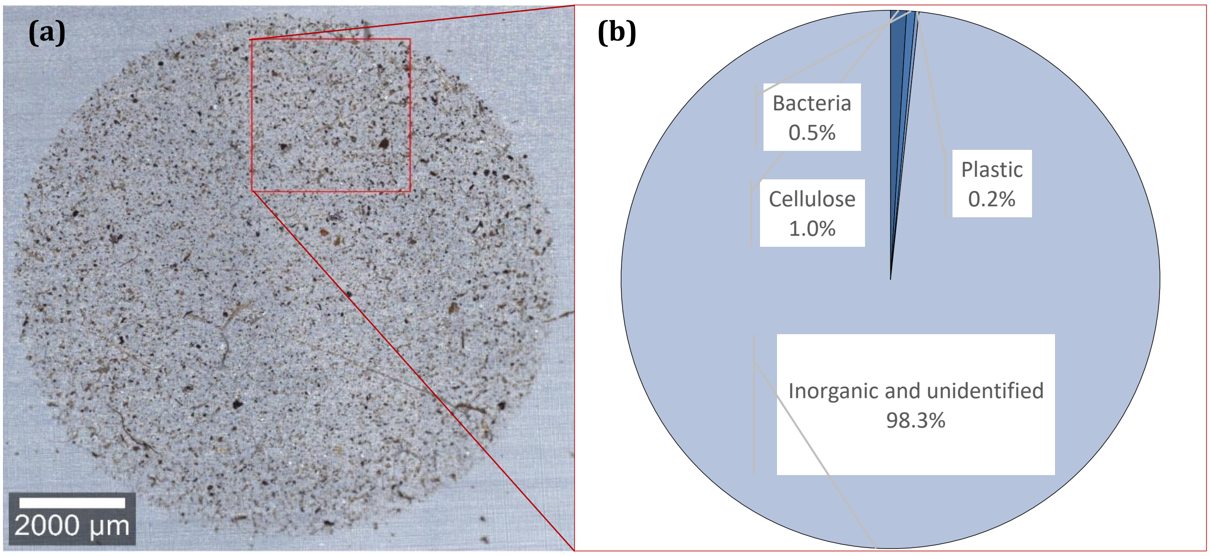

Figure S5a,b: (a) Optical stitching image of the filter and the selected area used for analysis *via* ParticleScout (3 × 3 mm^2); (b) distribution of particles on a subsample identified by ParticleScout. In total, 1362 particles were found by the WITec ParticleScout software, 3 particles were assigned to plastics, 13 to cellulose, and 7 to bacteria (*Escherichia coli* and *Corynebacterium glutamicum*).

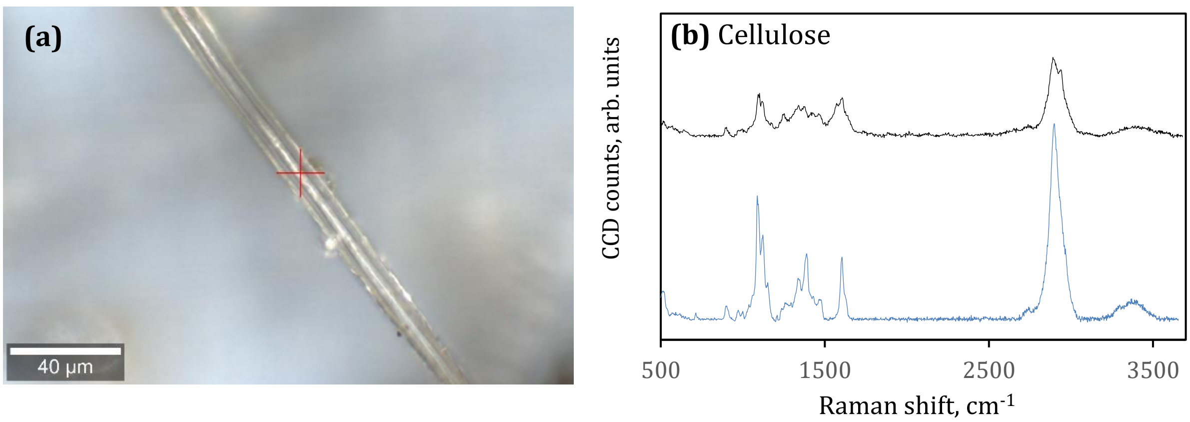

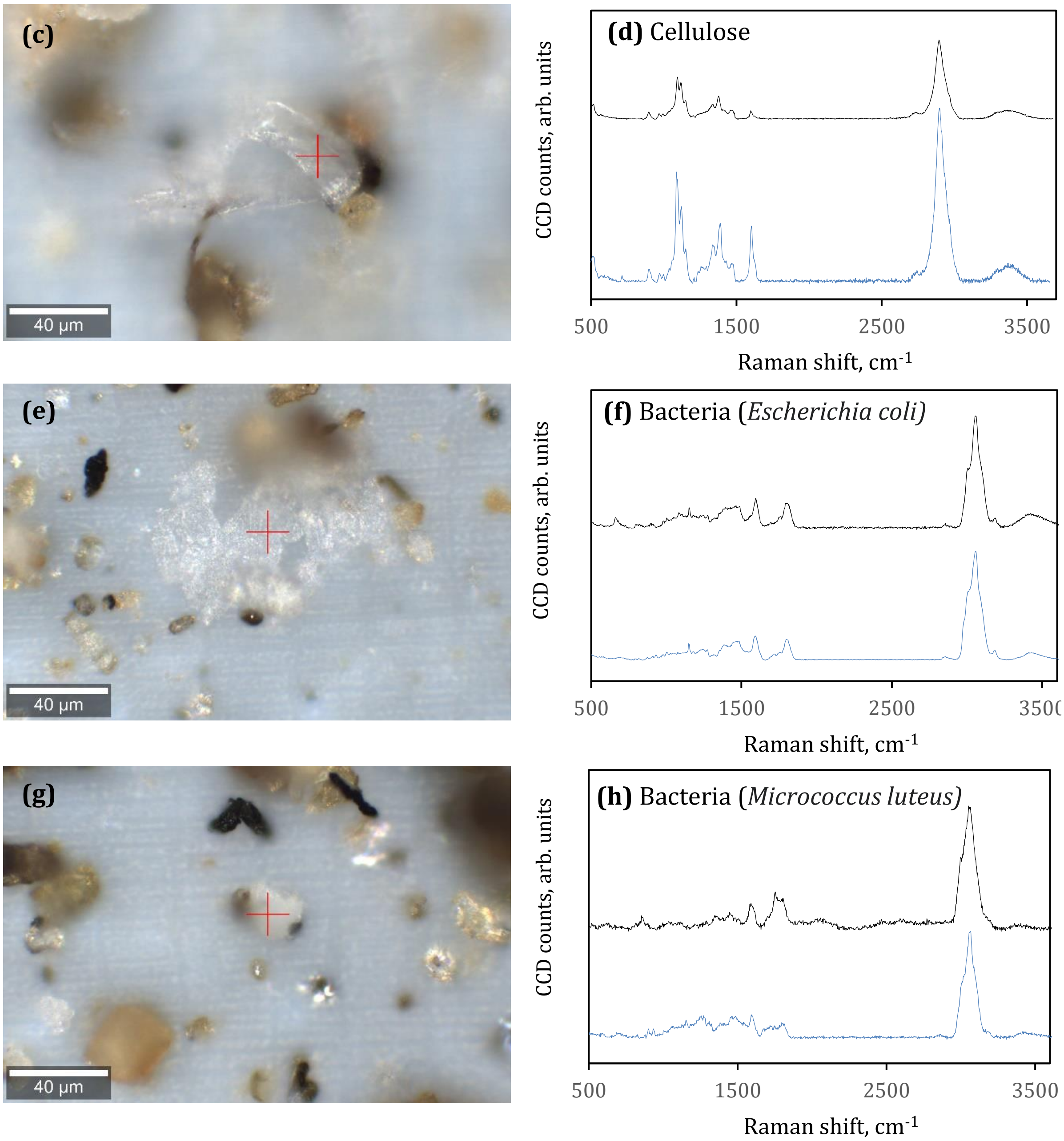

Figure S6a,h: (a,c) Optical images of cellulose particle fragments and (e,g) bacterial colonies, and (b, d, f, h) corresponding Raman spectra (black) in comparison with the reference spectra from the database (blue).

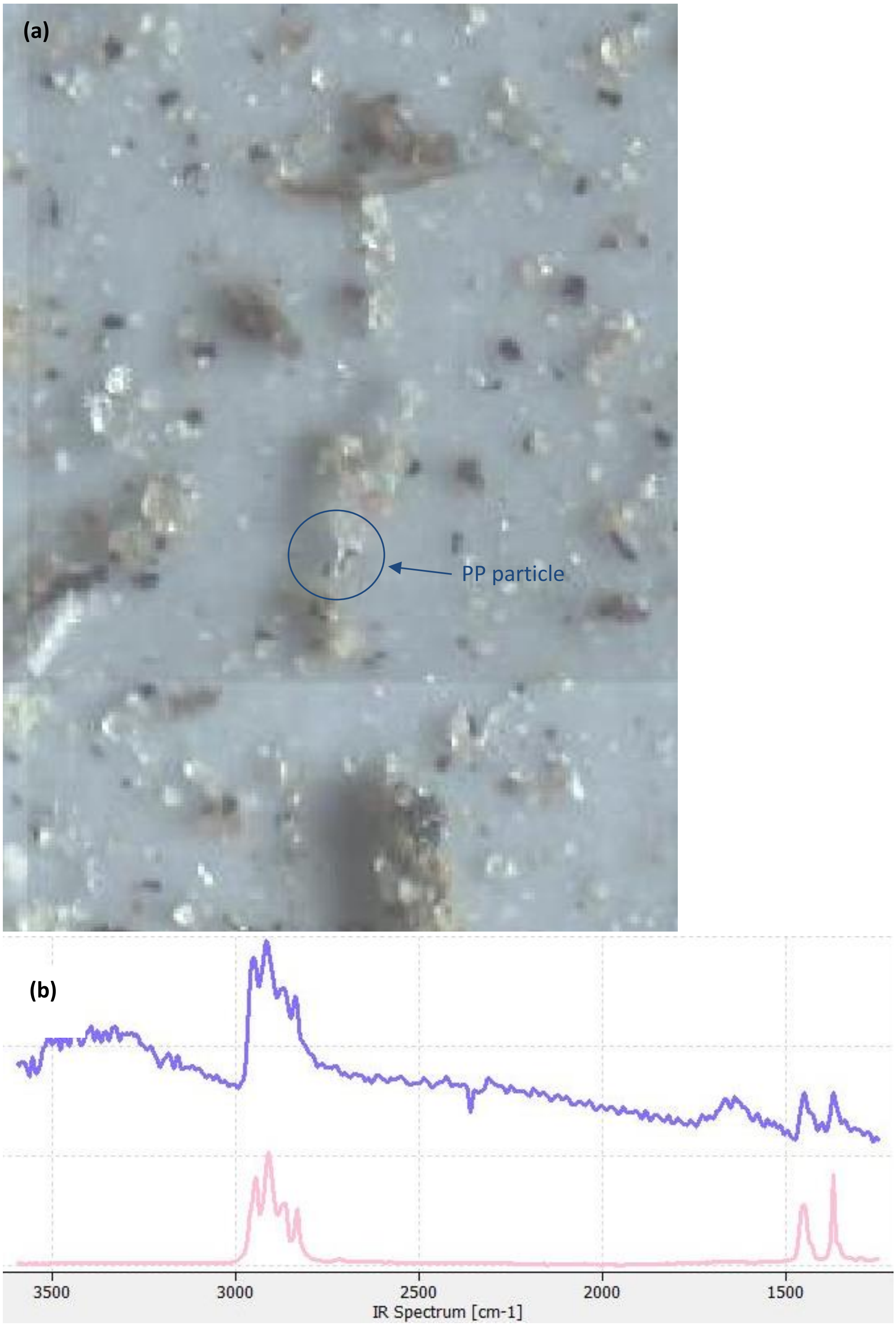

Figure S7a,b: (a) Optical image of filter fragment enclosing a polypropylene particle and (b) FTIR spectrum of the particle (purple) in comparison with the reference spectra (pink).

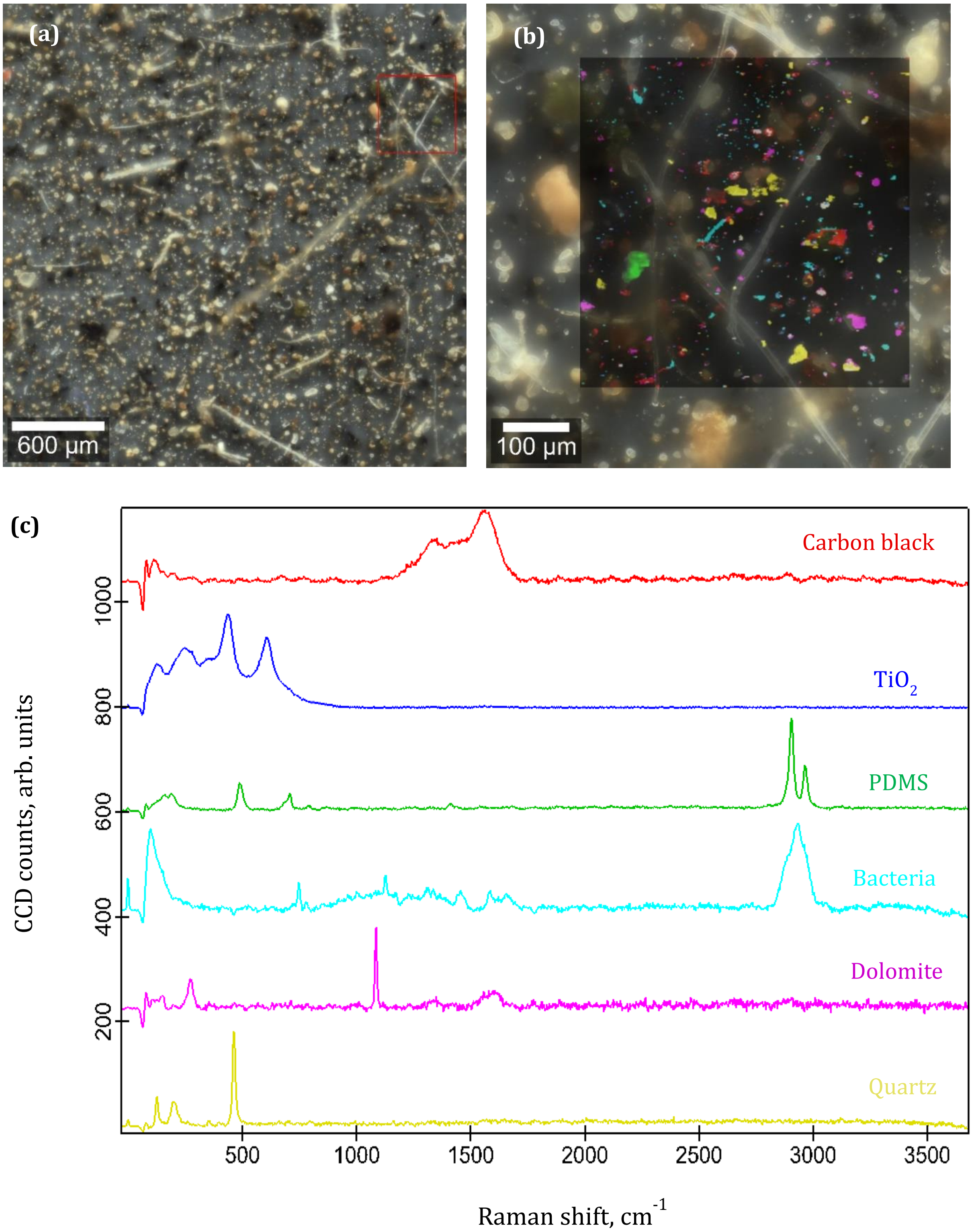

Figure S8a-c: (a) Optical stitching image of a filter fragment (corresponding to position 2 in Fig. 5a). The red square shows the position of the large area Raman scan (500 x 500 μm^2, step size of 2 μm pixel^{-1}), where a polydimethylsiloxane (PDMS) MP was found; (b) overlay of optical image with the component distribution obtained by True Component Analysis (Witec Project 5.3) of the large area Raman scan. Colour code corresponds to components, whose spectra are displayed in (c).

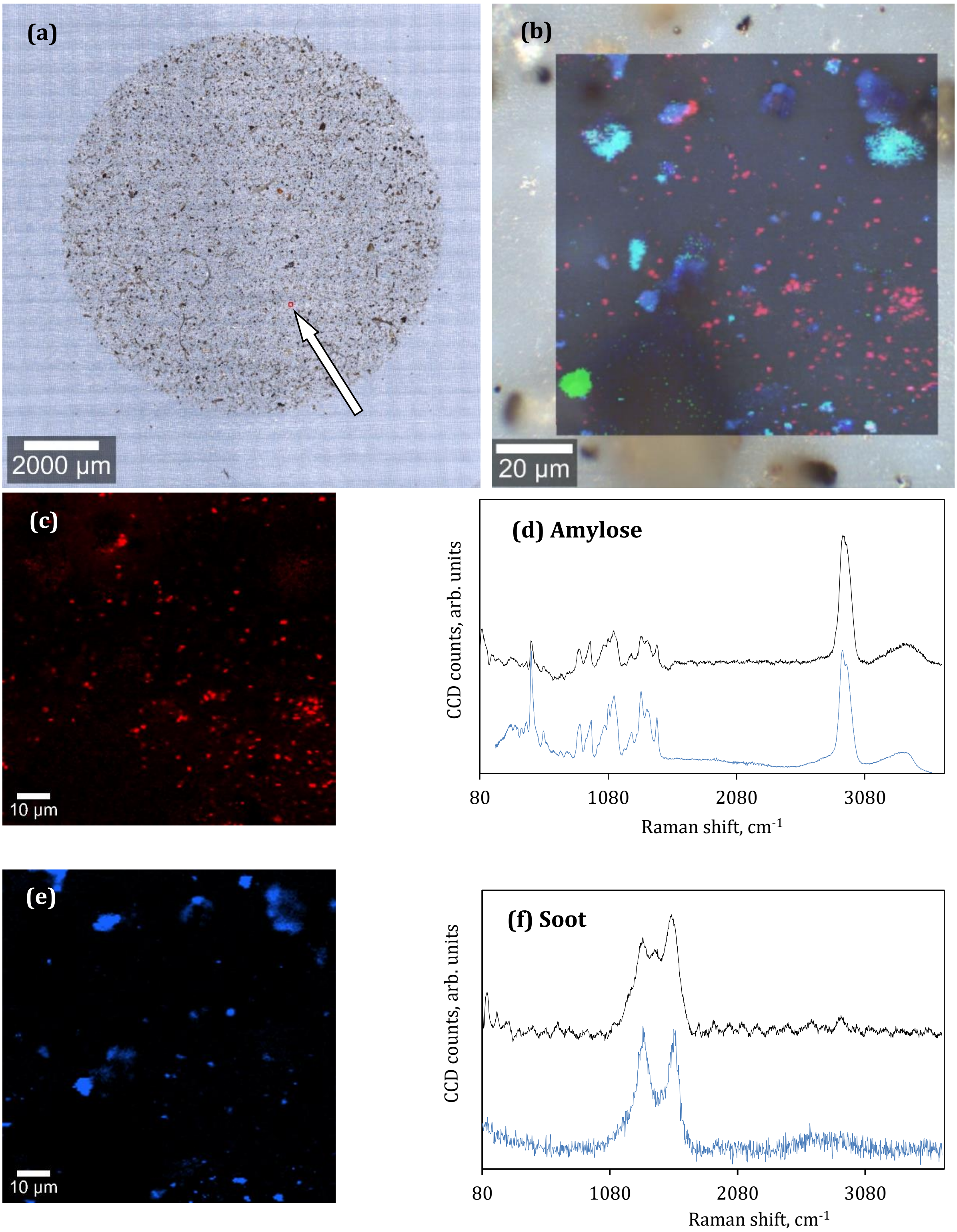

(a)
2000 µm
(b)
20 µm
(c)
10 µm
(d) Amylose
CCD counts, arb. units
80
1080
2080
3080
Raman shift, cm-1
(e)
10 µm
(f) Soot
CCD counts, arb. units
80
1080
2080
3080
Raman shift, cm-1

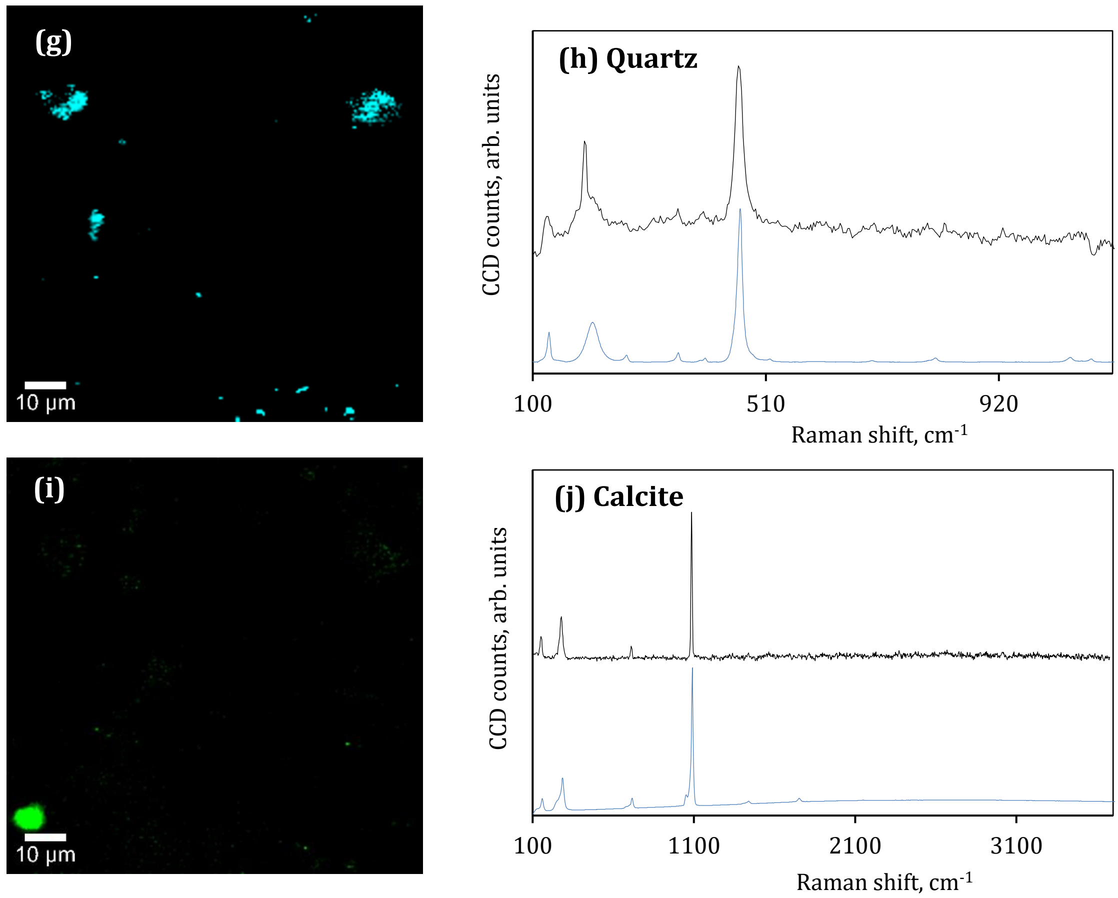

Figure S9a-j: (a) Optical stitching image of the filter indicating the position (red square) for the large area Raman scan (100 x 100 µm^2) conducted with a smaller step size of 0.5 µm pixel^{-1} (corresponding to position 3b in Fig. 5A); (b) overlay of optical image with component distribution retrieved from the large area Raman scan employing the True Component Analysis included in the Witec Project 5.3 software; spatial distributions of (c) amylose, (e) soot, (g) quartz, and (i) calcite particles and (d, f, h, j,) respective Raman spectra of the particles (black) extracted from True Component Analysis in comparison with the reference spectra from the database (blue).

References

1. Aluko O, Noll KE. Deposition and suspension of large, airborne particles. Aerosol science and technology. 2006;40:503–513.
2. Luft TA. Erste Allgemeine Verwaltungsvorschrift zum Bundes-Immissionsschutzgesetz (Technische Anleitung zur Reinhaltung der Luft–TA Luft). Vom. 2002;24:25–29.
3. Dioguardi F, Mele D, Dellino P, Dürig T. The terminal velocity of volcanic particles with shape obtained from 3D X-ray microtomography. Journal of Volcanology and Geothermal Research. 2017;329:41–53.
4. Saxby J, Beckett F, Cashman K, Rust A, Tennant E. The impact of particle shape on fall velocity: Implications for volcanic ash dispersion modelling. Journal of Volcanology and Geothermal Research. 2018;362:32–48.